International Journal of Pharmaceutics 397 (2010) 109–115

Contents lists available at ScienceDirect

International Journal of Pharmaceutics

journal homepage: www.elsevier.com/locate/ijpharm

Determining the coating thickness of tablets by chiseling and image analysis

Slobodan Šašić*

Pfizer, Global Research and Development, Groton, 06340 CT, USA

ARTICLE INFO

Article history:
Received 7 May 2010
Received in revised form 2 July 2010
Accepted 5 July 2010
Available online 17 July 2010

Keywords:
Coating thickness
Image analysis
Hill-climbing segmentation

ABSTRACT

Several tablets are chiseled and imaged in order to determine the variation in the coating thickness with the addition of the coating material (weight-gain). Chiseling is carried out with an ultrasonic chisel. The chiseled tablets are imaged in full and these images are exported into programming language Matlab in order to numerically analyze all the pixels along one side of the tablet. The coating thickness is statistically assessed at four cutting depths for three tablets obtained from four weight-gain experiments, a total of 48 images. The coating layer is clearly visible and determinable in the 'white-light' images even for the smallest weight gain of 1% but with sizeable errors due to the diffused boundaries between the coating and the core on one, and the coating and the background on the other side. Addition of the coating material clearly increases the coating thickness which is found to be somewhat higher at the top of the tablets than at the edges. Two approaches for assessment of the coating thickness are tested and are found to be in a very good agreement except for the thinnest coating layer.

1. Introduction

The tablets are often coated with materials that protect the core from the environmental effects and improve its cosmetic appearance or palatability (Kleinbach and Riede, 1995). For controlled-release formulations, the coating is one major factor that governs functionality of such products due to its influence on the rate of the release of the drug (Jantzen and Robinson, 2002). The thickness and porosity of the coating is its key feature. The most important element of the coating process is the amount of the coating material sprayed onto the cores which is usually represented through the weight-gain of the tablets. Satisfactory visual appearance of the tablets for the reasonably high weight-gain indicates the end of the coating. The actual homogeneity of the coating or its thickness may not even be considered for the immediate release formulations provided drug product performance tests are in line with expectations. For more complex or controlled-release formulations, a better insight into the coating is required which, it would seem, can easily be attained by imaging – the differences in the appearance of the coating and the core may be such to allow for clear visual separation under the microscope.

Limited literature references reporting on application of visual imaging for quantitative or semi-quantitative characterization of the coating are available. This technique has certainly been commonly applied as the simplest way to obtain immediate information on the thickness but, presumably, reading from the screen is deemed sufficient and the images are rarely processed. Various other physicochemical techniques are being used for this purpose. Chemical imaging based on vibrational (Ringqvist et al., 2003; Romero-Torres et al., 2006; Kauffman et al., 2007; Belu et al., 2008; Maurer and Leuenberger, 2009), X-ray (Barbash et al., 2009), or fluorescence spectroscopies (Andersson et al., 2000) are all applied for two-dimensional characterization of coated tablets. All these techniques are based on tagging specific analytical responses obtained by the above spectroscopies with the spatial coordinates on the sample. The amount and specificity of information obtained by these approaches often exceeds the need for simple recognition of the layers in the imaged material.

Technically, the most complex and hence of particular note are tomographic methods for three-dimensional representations of tablets. The very informative review by Zeitler and Gladden (2008) lists four key tomography methods that may be used for visually most impressive, non-invasive determination of coating thickness; terahertz imaging (TeraHz), X-ray microtomography (Ozeki et al., 2003; Traini et al., 2008), optimal coherence tomography (Stifter, 2007), and magnetic resonance imaging (Melia et al., 1998). TeraHz is apparently most often used for coating thickness determination as documented by a number of reports (Zeitler et al., 2007a,b; Ho et al., 2007; Ho et al., 2008) from the manufacturer of that instrument (TeraView).

The aim of this text is to use the simplest common instruments to create images with the core/coating boundary exposed and to quantitatively analyze these in order to assess variation in the coating thickness with the increase in weight-gain. In addition, the tablets are chiseled at several depths to evaluate the thickness variation across the length of the tablets. The emphasis here is on

* Tel.: +1 860 686 4180; fax: +1 860 686 5684.
E-mail address: slsasic@yahoo.com.

0378-5173/$ – see front matter © 2010 Elsevier B.V. All rights reserved.
doi:10.1016/j.ijpharm.2010.07.004

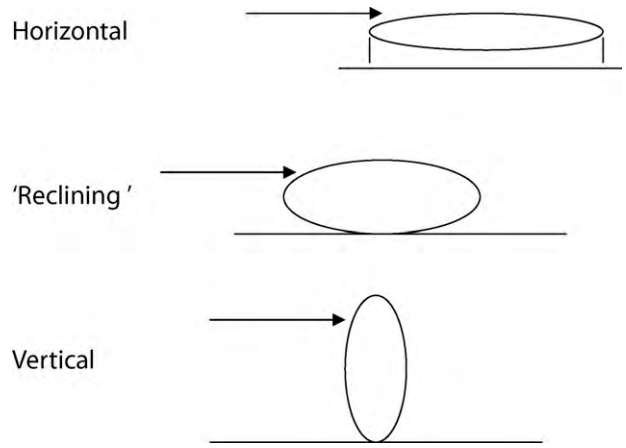

Fig. 1. Three possible positions for chiseling a tablet. The arrows mark possible chiseling directions.

analytical information and image-processing while the pharmaceutical aspects of the coating itself and the coating process are largely ignored. The intention is to provide an idea for an approach to be used as a process analytical tool (not as an online application though) and possibly for quality control. The industrial requirements are also given significant consideration here.

The content of this study is similar to the very recent work of Laksmana et al. (2009) who thoroughly analyzed the coating structure of various pellets (thickness, porosity, and pore size). Their paper is essentially a meticulous, quantitative imaging study in which the images of the pellets are obtained by confocal scanning laser microscopy, numerically enhanced, and then analyzed with various image-processing algorithms in order to describe the above parameters. The general idea of comprehensive image analysis for characterizing the coating is shared in both studies but the differences in the experiments and calculations are evident.

2. Experimental

The tablets are chiseled on an ultrasonic chisel device capable of chiseling in fine steps (10 μm) with the minimal initial cutting depth of 100 μm (custom made, Foster Miller, Waltham, MA, USA). The chiseling proceeds in a stepwise fashion with the fineness of lowering the blade depending on the desired final depth and the ability of the tablet to withstand the process. The instrument is entirely enclosed and equipped with a vacuum system for automated collection of dust so the whole process produces no contamination. The existing software-control is designed for much more complex operations than simple chiseling (which is not of interest for this application). The user only enters the final cutting depth and defines the step in which this depth is to be reached.

Tablets can generally be chiseled in three positions described in Fig. 1. The horizontal and vertical one are not considered suitable for this application for the following reasons: the vertical position is unsuitable due to the need for short but frequent chiseling in order to cover large areas on a tablet. In addition, there is a risk of the tablet being swept off the special slide on which it is mounted (simply glued to) due to the force of chiseling being applied to the position that is very distant from the glued part. The horizontal position is unsuitable too due to the need to completely remove the oval top of the tablet. If the concave top is not removed, which happens if the cutting depth is, for example, only 500 μm, the background in the image of the tablet is the same as the coating layer that is analyzed so the two are very hard to distinguish. This problem would not exist for a flat-top tablet. The 'reclining' position is thus chosen for all tablets, as it suffers much less from the effects described for the other two positions.

Three tablets from batches obtained from four weight-gain runs were chiseled, totaling 12.

Once chiseled, the tablets are moved (without ungluing) to an imaging-equipped microscope to collect images. The Perkin-Elmer Near-Infrared Mapping system 'Spotlight' is used for these purposes. This instrument is capable of collecting near-infrared spectra (and images) that can be used to identify chemical identity of the components in a tablet. Given this was of no importance for the current task, only normal microscopy images ('white-light', WL) are collected with it. 'Spotlight' is used in part due to convenience and, much more importantly, due to its ability to quickly collect WL images across large areas on the sample which is of crucial importance here. Normally, 10 mm × 10 mm images are collected which is the largest possible area coverage for this instrument. This allows for the whole tablet to be imaged which normally completes in about 10 min. Of course, any other microscope capable of imaging across large areas would suffice for this purpose.

The key parameter of the imaging system used for this application is its spatial resolution. The better the spatial resolution, the more accurate the thickness estimates. In this application, 8 μm is the size of each pixel in the image which is not very optimal with regards to the coating thicknesses analyzed (as will be shown later). However, when considered in light of the overall coverage of 10,000 μm × 10,000 μm, it is actually a rather good resolution.

An interesting observation here is that manually gluing a tablet for the holder before the chiseling may introduce some small errors that are detectable under the microscope. If the tablets are not glued 'perfectly' vertically to the holder, one of the sides may have larger shade of the coating than the other side rendering it hence less analyzable. This positioning error is practically unavoidable but normally it does not appear to have any significant effect on the measurements.

Given this study focuses on analytical and not pharmaceutical aspects of the coating, the details of the coating process are omitted. It suffices to say that the weight gain is varied from 1% to 4% in a routine spray drying coating procedure with Opadry II red coating. There is a sharp color difference between the coating and the core.

The obtained images (in the .bmp format) can be analyzed on the monitor of the microscope and also can be exported to apply more exact data analysis approaches.

Matlab (MatWorks, Natick, MA) is chosen as software support for the numerical analysis of the images. Essentially, all the operations with it were simple and did not require any particular routine to be created. Several lines executed separately sufficed to complete the analysis. Most of the images shown here were also produced in Matlab. Due to some of the results relying on the visual impression from the images, it needs to be said that the internal Matlab set-up for plotting images was not manipulated in any way.

It is also important to say that this programming language contains imaging toolbox with several routines that can be applied for automated image analysis (Laksmana et al., 2009). These algorithms are not used in this study however but instead a non-commercial algorithm downloaded from the Matlab-users-forum website (matlab.com, see references) is used for analysis of the images without operator's assistance. Details of this application are given in Section 4.

3. Results

The tablets are chiseled at four depths in order to provide information on the coverage along full length of one half of a tablet and not only at individual cross-sections. Although these four points obviously cannot replace the 3D perspective from a potential

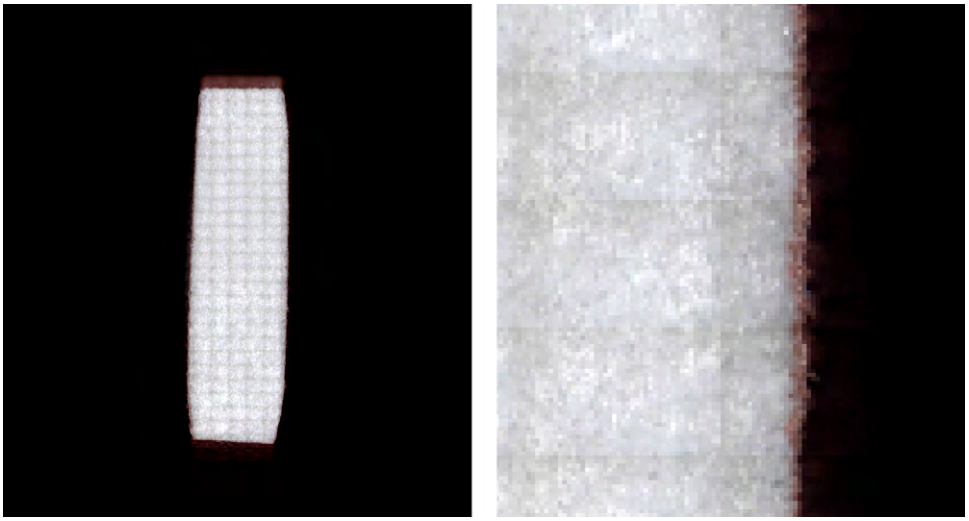

Fig. 2. An original 10 mm × 10 mm image of a 2% weight gain tablet cut at 500 μm (left). X8 enlargement of a small segment on the right-hand side of the tablet illustrating more clearly the visual appearance of the coating (right). Each pixel in these and all other images throughout is 8 μm.

tomography study on a whole tablet, they do contribute to better understanding of the coverage of a tablet.

Cutting depths of 0.5, 1, 1.5 and 2 mm are chosen. The last depth significantly cuts through the embossing and this causes some problems in estimating the coating thickness. However, the coating is confirmed abundantly present at the embossment so this problem only affects the calculations for describing the coating.

An example of an image (plotted in Microsoft Paint) obtained at the depth of 0.5 mm, 2% weight gain is given in Fig. 2. The coating is clearly visible and its thickness can be estimated by counting the associated (red) pixels. However, it is laborious to visually scroll through a very large number of pixels to analyze the whole length of the tablets.

By visually inspecting the sides of the tablet, one can approximately count the pixels belonging to the coating and hence assess the thickness as well as whether there is any unexpected variation in it (too thin or too thick). This is the most intuitive and certainly useful approach but it is subjective and quite coarse. No errors of the estimate and assessment of homogeneity can be obtained which is of importance given the thinness of the coating at the beginning of the process (at 1% weight gain), and also it is heavily dependent on the contrast of the software used for plotting.

Another approach is to try to automate the analysis of the pixels in the image. The idea here is to numerically analyze the actual values of the pixels. Every pixel in Fig. 2 has some associated intensity with the black background being zero. If the numerical difference between the white (core), the colored (coating), and the black pixels (background) is sufficient, then the colored pixels can be precisely identified in every row in the image. Having the exact numbers of coating-related pixels in each row allows for better estimates of the thickness across the whole edge of the tablet and of the related deviation.

In order to analyze the data in the proposed manner, the image in Fig. 2 is exported into software that can operate with the underlying numbers. Matlab is here used for such purposes and Fig. 3 is a Matlab presentation of Fig. 2 in a different color scale. What visually seems a determinable difference between the coat, coating, and background in Fig. 2 is somewhat smeared in Fig. 3. However, this is because Fig. 3 is a more accurate presentation of the data than Fig. 2 (i.e. Fig. 3 is an image of higher fidelity) in which the pixels values appear to be coarsely rendered.

According to the approach above, one would ideally like to have a three-step curve (Fig. 4) with the high value pixels associated with the core (e.g. the red pixels in Fig. 3), mid-value pixels associated with the coating (cyan), and zero pixels for the background (blue).

Such a situation is apparently not met in the one-dimensional presentation shown in Fig. 5 in which there is no sharp decrease in the values of the pixels at the boundary between the core and the coating as well as between the coating and the background. This is unsurprising because the image in Fig. 3 hints that such complications can occur, as it apparently contains more than three colors. It should be said here that the color palette for plotting an image is dependent on the internal criteria in the software used for plotting. For example, if there are less color levels, then an image contains better defined colors but this reduces the resolution and simply leads to a coarse rendering, while if there are too many color gradients, then an image may appear too colorful and hence confusing. The latter case is probably more acceptable as it does not extensively group the pixels and hence provides a better resolution.

Fig. 5 shows that there is a gradual transition between the core and the coating as well as between the coating and the background. The assignment of pixels associated to the coating is thus not trivial. The mid-value pixels are evident in Fig. 5 but one needs to set a

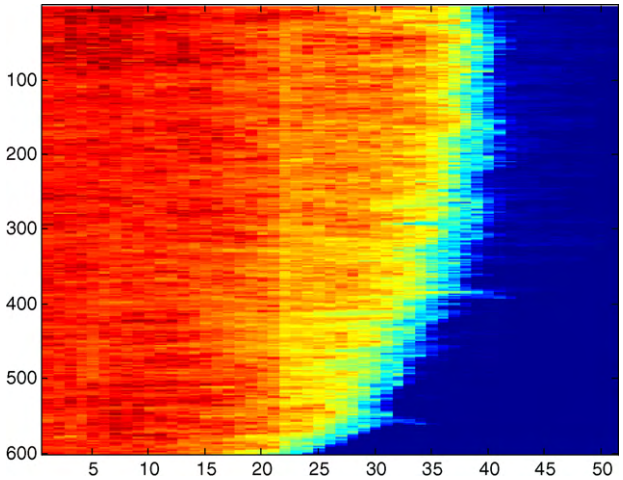

Fig. 3. Another random segment of 550 pixels in length (about 4.5 mm) from the left image in Fig. 2 plotted in Matlab. The differences between the core, the coating, and the background are more diffused in this presentation which is much finer than that in Fig. 2. The pixel sizes are not kept constant in this rendering that is very elongated along the abscissa. This is repeated through to aid visual comprehension.

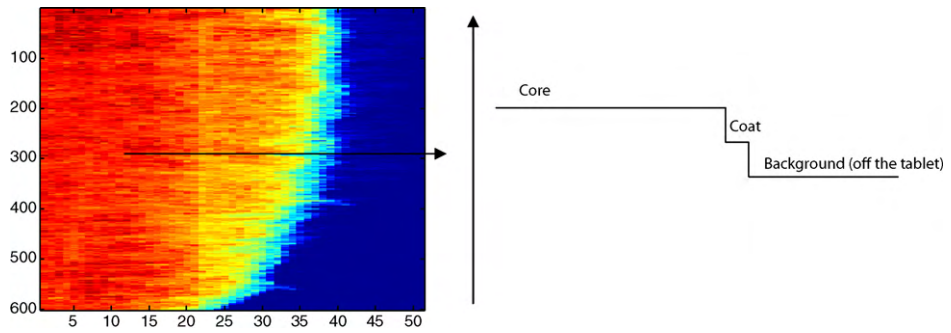

Fig. 4. Presentation of an ideal case for data analysis – the values of the pixels along the arrow should be high for the core, somewhat lower and relatively constant for the coating, and zero for the background. This would allow for easy counting of the pixels related to the coating. The colors in the image, however, suggest that the intensity variation is likely to be more gradual than in the scheme impeding thus straightforward counting of pixels. (Colors online only).

threshold to count them in each row of the image. This threshold should properly eliminate the pixels that are respectively, close to the core (too high) and the background (too low). Including these pixels would lead to overestimating the coating thickness.

The upper threshold criterion excludes the high-value pixels that slowly descent from the nearly constant values that represent the core (~0.06 in Fig. 5). This appears relatively simple to define due to high density of pixels at the boundary between the core and the coating – if the threshold is set to be at a too high value, a large number of such pixels would be counted leading to excessive values for thickness that would contradict the visual impressions from Figs. 3 and 5.

The bottom threshold was more difficult to define as the pixels values moderately decrease to reach the background and are not densely distributed. Setting a too low threshold would not produce so 'suspicious' thicknesses as it was the case for the upper threshold. Final decision is here based on the visual assessment of the deep blue pixels in Fig. 3 at the boundary between the coating and the background. These values are the experimental error as there can be no gradual transition between the core and the background as the latter refers to the empty slide. It is determined that the values below 0.015 in Fig. 5 are not likely to be associated with the coating and the threshold was thus set above it. Clearly, this criterion includes some subjectivity but it is not nearly as subjective as the full visual assessments of the images (described above). In addition, thresholding on such sparse distribution of pixels may (in most cases) lead to incorrectly assigning one pixel (i.e. overestimating thickness).

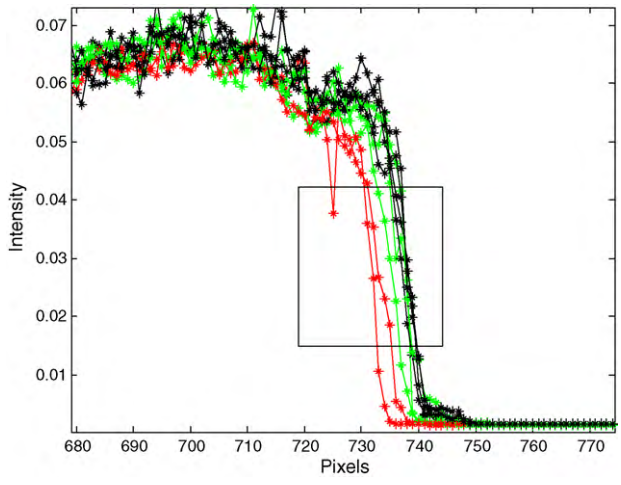

Fig. 5. One-dimensional presentation of the real data along several lines as that in Fig. 4. The difference between the core, the coating and the background is clear but gradual so a threshold for removing the pixels respectively too close to the core and the background has to be carefully defined. The shown rectangle corners the pixels considered to be the coating.

The rectangle in Fig. 5 thus defines the pixels associated with the coating, and these are counted and averaged. From each row in the image a single number can be obtained (coating thickness at that position) and plotting these values for all rows yields the overall homogeneity for the analyzed cutting depth. Variation of these numbers is the deviation in the coating thickness.

Fig. 6 demonstrates this approach for four cutting depths. For the high gain and the cutting depths of 0.5, 1 and 1.5 mm, the distribution of pixels (or, equivalently, the variation in the coating thickness) is very uniform and only occasional spikes can be noticed. There is no trend in the curves in Fig. 6 that would suggest one part of the tablet being better coated than the other. Interestingly, an obvious dent in the tablet due to embossing does not seem to significantly affect the coating thickness as there are no spikes associated with it. At the 2 mm cutting depth, the embossment is present all along the imaged area but the image is still analyzable. The embossment causes more frequent appearance of the spikes (due to the accumulation of the coating material) and also makes the tablets more susceptible to the appearance of artifacts. Therefore, the embossment certainly diminishes prospects of accurate analysis but does not prohibit application of the methodology described here.

The coating thicknesses determined via this method for three tablets at four cutting depths are summarized in Table 1.

The data from Fig. 6 show that the thickness of the coating is larger at the top of the tablet than at the edges. For the 3% and 4% weight gains the same coating thicknesses are essentially obtained – the difference between the two values is much smaller than the error of the average so according to this approach the coating process probably can be considered complete at the 3% weight gain. This holds not only for the global average of all values but also for the individual thicknesses at the individual cutting depths. In all likelihood, there should be a small difference between the coating thicknesses between the 4% and 3% weight gains but the applied methods are not sensitive enough to identify it.

The associated errors in pixel homogeneity appear very reasonable. Note that the minimal measurement error of one pixel corresponds to 8 μm. The numbers in Fig. 6 hence suggest that the applied image analysis introduces some additional errors but in turn it provides a comprehensive overview of the coating thickness across a large area on a tablet. The errors increase with the increase in the cutting depth due to the problems introduced by the embossment. When all the cutting depths are averaged however, the errors seem to remain constant, about 10 μm or somewhat more than one pixel. Despite being obtained on very different samples, many of these findings are similar to those reported by Laksmana et al. (2009).

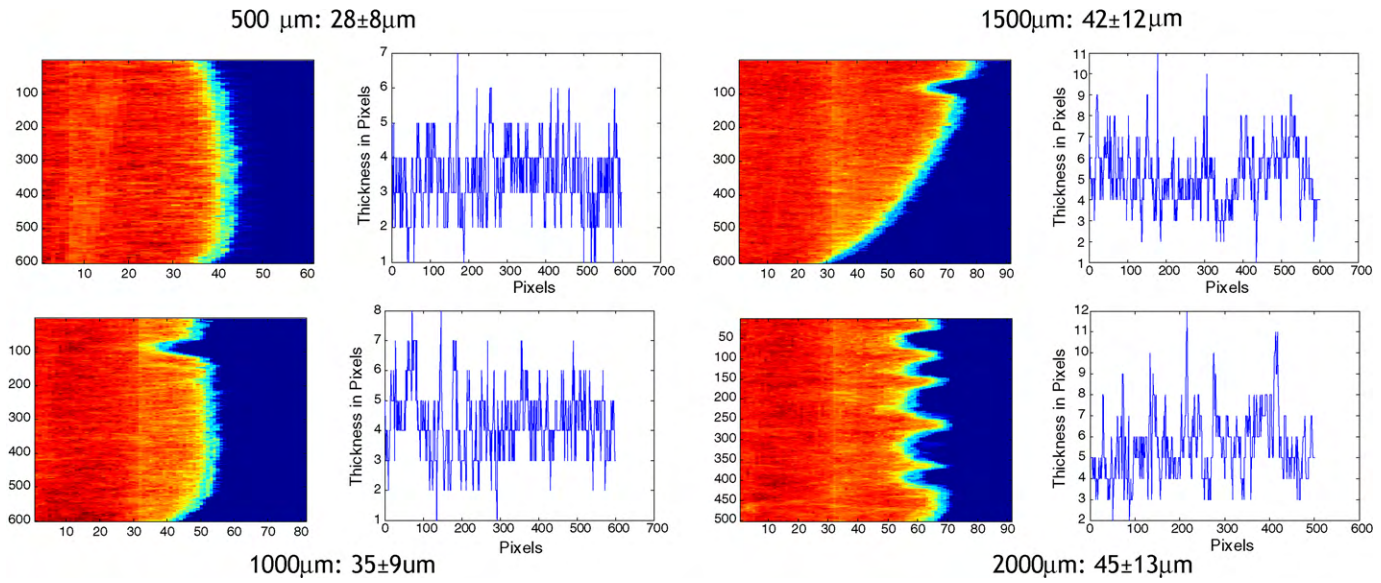

Fig. 6. Examples of the variation in the coating thickness for all four cutting depths. The thicknesses reported for various cutting depths are respectively obtained as the mean and standard deviations from the one-dimensional presentations that are obtained as illustrated in Figs. 4 and 5. The ordinates in these 1D plots are given in pixels with one pixel corresponding to 8 μm, while the abscissas correspond to the *Y*-axis in the images. The images differ because for each experiment the tablet is moved in and out of the microscope and no effort is made to analyze exactly the same area. Furthermore, the variation in the covered area is considered to be of no importance because the averages are calculated across large parts of tablets (~5 mm, or along ~600 pixels). The 2000 μm cutting depth passes across the embossment which negatively affects the flatness of the edge of the tablet and causes large variation in thickness due to the accumulation of the coating and some physical damage to the tablet in the course of chiseling.

4. Discussion and summary

With regards to the image analysis, the most desired situation would be to use an algorithm for automated decision on the boundaries on both sides of the coating. Such an algorithm would actually double-threshold the coating-related pixels which is not a trivial operation and related software may not be easily accessible. This type of image-segmentation problem is frequently encountered in computer vision. While detailing on it is clearly beyond the scope of this study, an application of one of the computational approaches in that field is warranted and comparing its results with the above operator-assisted thresholding is certainly valuable. Here, so-called 'Hill-climbing' approach (Russell and Norvig, 2003) is tested via the 'HillClimbingSegment' function kindly shared by its author from the Nanyang Technological University, China, and freely downloadable from the Matlab-users-forum (http://www.mathworks.com/matlabcentral/fileexchange/22274 and references on that page).

Briefly, 'HillClimbingSegment' transforms an image (normally a 3D array) into a more analyzable form and then provides the seeds for the k-means method to determine the clusters of pixels in it. Once the pixels are classified through the k-means, they are reverted back to form an image that is now transformed into a combination of clusters. This leads to a significant simplification of the visual appearance with one color per cluster (the same effect is achieved with counting the pixels between the thresholds defined in Fig. 5). In this case, the acceptable outcome is a three-color image in which the coating part is to be analyzed and its parameters compared with the data in Table 1.

The software used has only one input that determines the internal re-arrangement (binning) of the data before the seeding and clustering are executed and image reformed. Depending on this

Table 1
Summary of the coating thicknesses for the three tablets at four weight gains, cut at four depths. The 2000 μm cut for 1% gain produced erratic results due to the thin coating crumbling during the chiseling. The results are given in microns as mean ± standard deviation (std).

Cutting depth (μm)		1% Gain		Overall mean ± std
500	20 ± 10	20 ± 10	19 ± 9	
1000	25 ± 10	25 ± 11	27 ± 12	23 ± 11 (500 and 1000 only)
1500	30 ± 13	29 ± 14	31 ± 12	
2000	–	–	–	
		2% gain		
500	19 ± 8	27 ± 9	27 ± 10	
1000	25 ± 12	34 ± 11	32 ± 12	33 ± 12
1500	34 ± 13	39 ± 12	38 ± 16	
2000	33 ± 13	36 ± 15	36 ± 14	
		3% gain		
500	34 ± 9	33 ± 8	33 ± 8	
1000	37 ± 8	39 ± 11	38 ± 9	40 ± 10
1500	44 ± 11	43 ± 10	41 ± 12	
2000	46 ± 15	44 ± 12	47 ± 13	
		4% gain		
500	30 ± 9	28 ± 8	33 ± 7	
1000	35 ± 9	35 ± 9	38 ± 9	39 ± 11
1500	42 ± 11	42 ± 12	41 ± 11	
2000	45 ± 13	45 ± 13	47 ± 17	

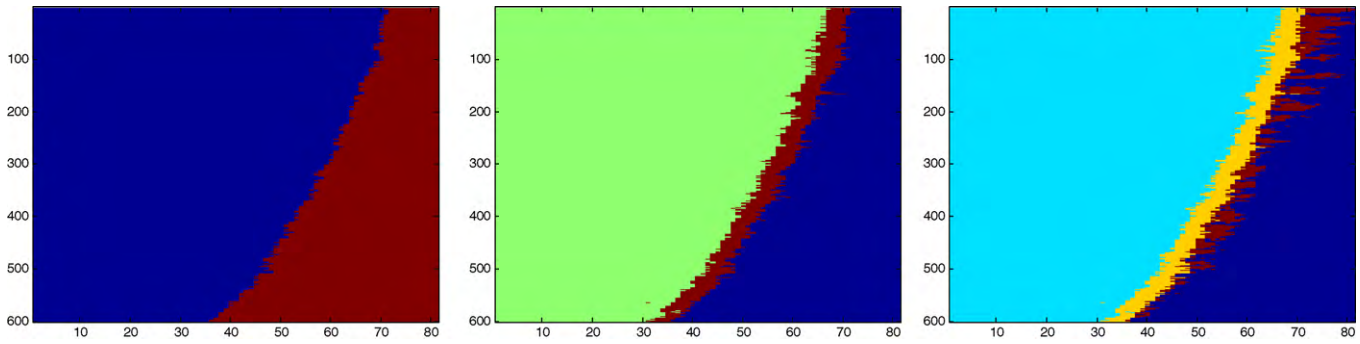

Fig. 7. Several outputs from an application of a Hill-climbing algorithm for segmenting images ('HillClimbingSegment'). The middle image corresponds to the real physical situation. The parameters of the layer next to the core in the four-layers image are practically the same as of the corresponding layer in the middle image so the presence of the fourth layer may be considered an ignorable mathematical artifact (although this must be checked on a case-by-case basis). As above, each pixel on the axes stands for 8 microns, with the elongation along the abscissa.

parameter, several outcomes are possible, as described in Fig. 7. Apparently, one of these images corresponds to the expectation while the rest contains too many or too few layers. Presence of too many layers, however, does not necessarily signify a failure of the analysis. For example, the parameters of the coating layer (mean and std) are the same for the three- and four-layers images in Fig. 7 so the fourth layer simply relates to inaccuracies in clustering the background and not the coating layer.

Comparison between the results from Table 1 and those obtained by 'HillClimbingSegment' routine are given in Table 2 for several tablets. In general, the agreement is excellent for both means and std-s for most of the images (above 500 μm cutting depth for 2–4% weight gain). With the increase in the thickness the numerical definition of the layers becomes more favorable for analysis resulting hence in a very good agreement between the two approaches. For the less-well defined layers, there are differences and occasionally HillClimbing-based algorithm fails to recognize layers in the tablet in a meaningful way. This mostly refers to the 500 μm cutting depth and low weight gain. Such samples were characterized with relatively large errors in Table 1 too so it is not surprising to find discrepancies here. In conclusion, there is a very good agreement between the fully automated software for determining the layers and the described vision-based approach leading to promising options for fully automated, no operator-assisted analysis.

Principal component analysis (PCA), a well-known and often applied statistical method in various fields of science, is tested here too with the idea that the cluster of mid-range points may be described by a single principal component leading to a separate image of the coating layer. Attempts with several raw images proved to be surprisingly unsuccessful. Nothing even remotely similar to Fig. 7 emerged from PCA.

With regards to the hardware, the key positive characteristics of the method described here are its simplicity and (very) low cost. Every step in the analysis is firmly and reliably controlled with very transparent results which thus can serve as a standard for comparison in case more advanced methodologies (such as X-ray or TeraHz tommography) are employed in parallel. The key negatives are obvious – it is a manual approach, destroys the samples, and does not provide a 3D perspective. In fairness though, it should be said that 'manual' here actually does not involve any labor or attendance of the operator.

The cutting is trivial to conduct and any chiseling instrument can be used to section the tablets (the ultrasonic chisel employed here is actually manufactured for specific purposes that go far beyond simple cutting). The exact cutting depth may be of no importance. Here, it was possible by default to precisely determine the cutting depths but cutting at arbitrary depths may be quite sufficient, depending on the sophistication of the analyzed material. Clearly, the coating layer in tablets is just one possible application amongst various other layered materials in pharmaceutical industry (such as beads and functional coatings).

The microscopy is also easily carried out and the obtained images can be exported and analyzed by the most efficient software tools and not only visually assessed.

Finally, the key element of the approach here is the automated image analysis. The relatively simple clustering problem met here may be swiftly addressed by an imaging expert familiar with such applications. Frequent usage in an industrial environment would, however, require routines such as the algorithm described here that are user-friendly and simply executable. 'HillClimbingSegment' routine proved to answer both of these and presented itself as a possible solution for automating image analysis. Even in the absence of such software, as thoroughly described above, quite simple, Matlab-based determination of thresholds without using any particular algorithm may lead to comprehensive image analysis. Therefore even without further refinements on this matter, which are certainly attainable, there

Table 2
Comparison of coating thicknesses for some tablets (in microns) in Table 1 with those obtained via using Hill-climbing-based algorithm for completely automated determination of layers.

Cutting depth (μm)	From Table 1	2% Gain Via segmentation algorithm	From Table 1	Via segmentation algorithm
500	19 ± 8	24 ± 10	27 ± 9	33 ± 10
1000	25 ± 12	27 ± 11	34 ± 11	34 ± 11
1500	34 ± 13	–	39 ± 12	38 ± 10
2000	33 ± 13	33 ± 16	36 ± 15	37 ± 15
		3% Gain		
500	34 ± 9	37 ± 8	33 ± 8	40 ± 10
1000	37 ± 8	37 ± 8	39 ± 11	38 ± 12
1500	44 ± 11	42 ± 9	43 ± 10	43 ± 11
2000	46 ± 15	46 ± 16	44 ± 12	44 ± 12

is a very good prospect for minimally subjective image analysis.

The combination of the three elements (chisel, microscope, software), leads to a quick and inexpensive assessment of the coating thickness. In an optimized/well established process, it should take several minutes to respectively chisel, image, and analyze.

The same tablets were also analyzed by the X-ray and TeraHz tomography. Preliminary comparison shows very good agreement between the X-ray data and chisel/image analysis while the TeraHz technology could not be purposefully employed due to the layer thickness being below its limit of detection.

References

Andersson, M., Holmquist, B., Lindquist, J., Nilsson, O., Wahlund, K.-G., 2000. Analysis of film coating thickness and surface area of pharmaceutical pellets using fluorescence microscopy and image analysis. J. Pharm. Biomed. Anal. 22, 325–339.

Barbash, D., Fulghum, J.E., Yang, J., Felton, L., 2009. A novel imaging technique to investigate the influence of atomization air pressure on film-tablet interfacial thickness. Drug Dev. Ind. Pharm. 35, 480–486.

Belu, A., Mahoney, C., Wormuth, K., 2008. Chemical imaging of drug eluting coatings: combining surface analysis and confocal Raman microscopy. J. Controlled Release 126, 111–121.

Hill-climbing based approach: http://www.mathworks.com/matlabcentral/fileexchange/22274.

Ho, L., Müller, R., Römer, M., Gordon, K.C., Heinämäki, J., Kleinebudde, P., Pepper, M., Rades, T., Shen, Y., Strachan, C.J., Taday, P., Zeitler, J.A., 2007. Analysis of sustained-release tablet film coats using terahertz pulsed imaging. J. Controlled Release 119, 253–261.

Ho, L., Müller, R., Gordon, K.C., Kleinebudde, P., Pepper, M., Rades, T., Shen, Y., Taday, P.F., Zeitler, J.A., 2008. Applications of terahertz pulsed imaging to sustained-release tablet film coating quality assessment and dissolution performance. J. Controlled Release 127, 79–87.

Jantzen, G.M., Robinson, J.R., 2002. In: Banker, G.S., Rhodes, C.T. (Eds.), Sustained and Controlled-release Drug Delivery Systems in Modern Pharmaceutics. Marcel Dekker, New York.

Kauffman, J.F., Dellibovi, M., Cunningham, C.R., 2007. Raman spectroscopy of coated pharmaceutical tablets and physical models for multivariate calibration to tablet coating thickness. J. Pharm. Biomed. Anal. 43, 39–48.

Kleinbach, E., Riede, T., 1995. Coating of Solids. Chem. Eng. Process. 94, 04021-4.

Laksmana, F.L., Van Vliet, L.J., Hartman Kok, P.J.A., Vromans, H., Frijlink, H.W., Van der Voort Maarschalk, K., 2009. Quantitative image analysis for evaluating the coating thickness and pore distribution in coated small particles. Pharm. Res. 26, 965–976.

Maurer, L., Leuenberger, H., 2009. Terahertz pulsed imaging and near infrared imaging to monitor the coating process of pharmaceutical tablets. Int. J. Pharm. 370, 8–16.

Melia, C.D., Rajabi-Siahboomi, A.R., Bowtell, R.W., 1998. Magnetic resonance imaging of controlled release pharmaceutical dosage forms. Pharm. Sci. Technol. Today 1, 32–39.

Ozeki, Y., Watanabe, Y., Inoue, S., Danjo, K., 2003. Comparison of the compression characteristics between new one-step dry-coated tablets (OSDRC) and dry-coated tablets (DC). Int. J. Pharm. 259, 69–77.

Ringqvist, A., Taylor, L.S., Ekelund, K., Ragnarsson, G., Engstrom, S., Axelsson, A., 2003. Atomic force microscopy analysis and confocal Raman microimaging of coated pellets. Int. J. Pharm. 267, 35–47.

Romero-Torres, S., Perez-Ramos, J.D., Morris, K.R., Grant, E.R., 2006. Raman spectroscopy for tablet coating thickness quantification and coating characterization in the presence of strong fluorescent interference. J. Pharm. Biomed. Anal. 41, 811–819.

Russell, S.J., Norvig, P., 2003. Artificial Intelligence – A Modern Approach. Prentiss Hall, Upper Saddle River, NY, USA.

Stifter, D., 2007. Beyond biomedicine: a review of alternative applications and developments for optical coherence tomography. Appl. Phys. B Lasers Opt. 88, 337–357.

Traini, D., Loretit, G., Jones, A.S., Young, P., 2008. X-ray computed microtomography for the study of modified release systems. Micros. Anal. 22, 13–17.

Zeitler, J.A., Gladden, L.F., 2008. In-vitro tomography and non-destructive imaging at depth of pharmaceutical solid dosage forms. Eur. J. Pharm. Biopharm. 71, 2–22.

Zeitler, J.A., Taday, P.F., Newnham, D.A., Pepper, M., Gordon, K.C., Rades, T., 2007a. Terahertz pulsed spectroscopy and imaging in the pharmaceutical setting – a review. J. Pharm. Pharmacol. 59, 209–223.

Zeitler, J.A., Shen, Y.C., Baker, C., Taday, P.F., Pepper, M., Rades, T., 2007b. Analysis of coating thickness, structure and uniformity in solid oral dosage forms by 3D terahertz pulsed imaging. J. Pharm. Sci. 96, 330–340.